frontiers | Frontiers in Chemistry

TYPE Original Research
PUBLISHED 28 October 2022
DOI 10.3389/fchem.2022.996604

OPEN ACCESS

EDITED BY
Jianrong Xu,
Shanghai University of Traditional Chinese Medicine, China

REVIEWED BY
Ping Yu,
Shanghai Jiao Tong University, China
Changlin Liu,
Central China Normal University, China

*CORRESPONDENCE
Hongli Wu,
Hongli.wu@unthsc.edu
Kayla N. Green,
kayla.green@tcu.edu

†These authors have contributed equally to this work and share senior authorship

SPECIALTY SECTION
This article was submitted to Chemical Biology, a section of the journal Frontiers in Chemistry

RECEIVED 18 July 2022
ACCEPTED 05 October 2022
PUBLISHED 28 October 2022

CITATION
Zhang J, Yu Y, Mekhail MA, Wu H and Green KN (2022), A macrocyclic molecule with multiple antioxidative activities protects the lens from oxidative damage.
Front. Chem. 10:996604.
doi: 10.3389/fchem.2022.996604

A macrocyclic molecule with multiple antioxidative activities protects the lens from oxidative damage

Jinmin Zhang[1], Yu Yu[1], Magy A. Mekhail[2], Hongli Wu[1,3*†] and Kayla N. Green[2*†]

[1]Pharmaceutical Sciences, College of Pharmacy, University of North Texas Health Science Center, Fort Worth, TX, United States, [2]Department of Chemistry and Biochemistry, Texas Christian University, Fort Worth, TX, United States, [3]North Texas Eye Research Institute, University of North Texas Health Science Center, Fort Worth, TX, United States

Growing evidence links oxidative stress to the development of a cataract and other diseases of the eye. Treatments for lens-derived diseases are still elusive outside of the standard surgical interventions, which still carry risks today. Therefore, a potential drug molecule $^{OH}Py_2N_2$ was explored for the ability to target multiple components of oxidative stress in the lens to prevent cataract formation. Several pathways were identified. Here we show that the $^{OH}Py_2N_2$ molecule activates innate catalytic mechanisms in primary lens epithelial cells to prevent damage induced by oxidative stress. This protection was linked to the upregulation of Nuclear factor erythroid-2-related factor 2 and downstream antioxidant enzyme for glutathione-dependent glutaredoxins, based on Western Blot methods. The anti-ferroptotic potential was established by showing that $^{OH}Py_2N_2$ increases levels of glutathione peroxidase, decreases lipid peroxidation, and readily binds iron (II) and (III). The bioenergetics pathway, which has been shown to be negatively impacted in many diseases involving oxidative stress, was also enhanced as evidence by increased levels of Adenosine triphosphate product when the lens epithelial cells were co-incubated with $^{OH}Py_2N_2$. Lastly, $^{OH}Py_2N_2$ was also found to prevent oxidative stress-induced lens opacity in an *ex vivo* organ culture model. Overall, these results show that there are multiple pathways that the $^{OH}Py_2N_2$ has the ability to impact to promote natural mechanisms within cells to protect against chronic oxidative stress in the eye.

KEYWORDS

$^{OH}Py_2N_2$, lens, oxidative stress, Nrf2, glutaredoxin, ferroptosis

Introduction

Cataracts are the most common cause of vision loss in individuals over the age of 60 as well as the leading cause of blindness in the world. According to the latest assessment from the World Health Organization, more than half of the cases of blindness worldwide are attributed to cataracts (Organization, 2019). Moreover, the trend toward an increased

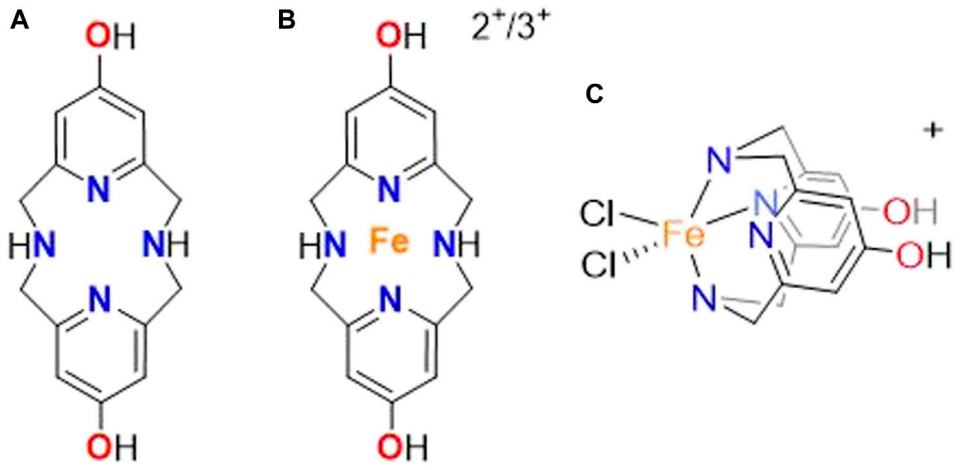

FIGURE 1
Structure of the **(A)** $^{OH}Py_2N_2$ molecule along with the connectivity of the **(B)** iron (II) and (III) complex and **(C)** orientation of the iron in the $^{OH}Py_2N_2$ ligand based on UV-vis studies.

aging population has built global attention to reducing the prevalence of cataract. Currently, the only treatment option to correct a cataract patient's vision is surgery. Though cataract surgery is a well-established procedure, complications may still arise, especially in patients of advanced age. Surgery-related complications such as posterior capsular opacity, intraocular lens dislocation, eye inflammation, photopsia, ocular hypertension, and macular edema may cause irreversible blindness (Chan et al., 2010). Therefore, there is still a great need to identify non-surgical therapeutic options with benefits outweighing the risks of surgery.

Oxidative stress encompasses a range of deficiencies in the balance between pro-oxidant and antioxidant regulatory pathways and the related damage to biological structures (Naik et al., 2014; Czerska et al., 2015). The eye is a prominent target of oxidative stress. It is continuously exposed to various oxidative conditions, such as photo-oxidation, ultraviolet (UV) radiation, smoke, and various forms of pollutants. Thus, oxidative stress has been associated with many ocular disorders, notably age-related macular degeneration (AMD) and cataracts (Spector, 1995; Beatty et al., 2000; Lou, 2003; Yildirim et al., 2011). Chronic exposure to light from the Sun, the largest source of UV radiation in our environment, can significantly increase the risk of a cataract, particularly if the recipient is over 40 years of age (Wolff, 1994). Solar UV that penetrates the atmosphere is mainly composed of UVA (320–400 nm) and UVB (290–320 nm) radiation (Zigman, 1995). This strong UV energy induces overproduction of reactive oxygen species (ROS) that damage lens epithelial cells (LECs), disturb the energy metabolism pathways, promote insoluble protein aggregation, and eventually lead to lens opacity (Lofgren, 2017). Therefore, the need to rebalance ROS to prevent chronic disease like this in the eye continues to be a driving force for the development of new, targeting molecules and studies to understand the mechanisms of their action(s).

Creating interventions for uncontrolled ROS is challenging, but there is strong evidence that antioxidant approaches to prevent or curb disease have positive impacts and show this is a feasible approach (Pisoschi et al., 2021; Woo et al., 2014; Bosco et al., 2011; DeCensi et al., 2010; Goodson et al., 2009; Zhang, 2019; D'Souza et al., 2020; Nechuta et al., 2011; Sotgia et al., 2011; Giem et al., 1993; Fraser, 2009; Singh et al., 2003; Cooper et al., 2009; Zhang et al., 2014a; Farrawell et al., 2018; Rowe et al., 2020; Ikawa et al., 2015; Williams et al., 2016). For example, the Age Related Eye Disease Study sponsored by the National Eye Institute strongly support that high levels of antioxidant vitamins and zinc can reduce the risk of advanced AMD and its associated vision loss (Age-Related Eye Disease Study Research Group, 2001; Chew et al., 2013). Nevertheless, there remains a gap between the current understanding of oxidative stress in disease pathologies and the development of new therapeutic molecules that successfully target this etiology (Lannfelt et al., 2008; Alzheimer's Disease Facts, 2016; Jarvis, 2015; Ratner, 2015; Niedzielska et al., 2016; Doig et al., 2017; Kingwell, 2017; Crielaard et al., 2017; Patel, 2016). During drug design for a disease, therapeutics are typically targeted toward one causative agent ex: cholesterol, an enzyme, or gene. However, such an approach is complicated for diseases involving oxidative stress because the etiology of oxidative stress is multifactorial. Identification of a therapeutic agent that can target multiple antioxidant pathways or induce defense mechanisms innate to the cell could prove powerful in fighting these diseases.

As a result of the current challenges for diseases that involve oxidative stress, we designed the $^{OH}Py_2N_2$ multimodal small molecule (Figure 1) with direct targeting reactivity against ROS (Johnston et al., 2019). Several benchtop assays validated our initial hypothesis that the water soluble molecule could function as a direct antioxidant molecule. Integration of a hydroxyl substituted pyridine group within a tetra-aza macrocyclic ring generates the $^{OH}Py_2N_2$ small molecule that can readily scavenge free radicals as well as bind mis-regulated transition metal ions, halting toxic metal redox processes (Green et al., 2019; Johnston et al., 2019). Interestingly and not part of our initial design, which focused on direct reactivity with ROS, $^{OH}Py_2N_2$ showed the potential to activate cellular antioxidant defense capacity *via* activation of the Nrf2 (Nuclear factor erythroid 2-related factor 2) signaling pathway in neuronal cell culture along with low toxicity, high metabolic stability, and proving to be highly water soluble (Johnston et al., 2019). Nrf2 is a transcription factor that plays key roles in antioxidant and detoxification responses, particularly in the eye. Nrf2 activates more than 250 antioxidant enzymes and pro-survival genes (Ma, 2013). It is commonly referred to as the gatekeeper to coordinated induction of cytoprotective and antioxidant genes or master antioxidant transcriptional regulator (Kaspar et al., 2009). Increased Nrf2 activity correlates with cellular survival and protection from oxidative injury to RPE cells and pathogenic processes (Johnson et al., 2009; Zhang et al., 2014b; Cuadrado et al., 2018; Tang et al., 2018; Bahn et al., 2019; Han et al., 2019; Kitaoka et al., 2019; Sotolongo et al., 2020). Likewise, lower Nrf2 expression is associated with an increased risk or early onset of diseases of the eye (Zhao et al., 2011; von Otter et al., 2010). Therefore, activation of Nrf2 pathways has garnered significant interest as a potential target for therapeutic design. The ability for $^{OH}Py_2N_2$ to activate this pathway piqued our interest to further explore the catalytic (enzyme based) and cellular pathways that this molecule might unlock to provide protection against oxidative stress.

The recently established understanding of the direct antioxidant activity of $^{OH}Py_2N_2$ through radical and transition metal scavenging, along with preliminary results suggesting catalytic protection *via* the Nrf2 pathway prompted the present studies focused on the therapeutic potential and activation of defensive antioxidant mechanisms induced by $^{OH}Py_2N_2$ to protect against oxidative stress in the eye (Johnston et al., 2019). To explore this potential, human lens epithelial cells were exposed to conditions that model oxidative stress and showed excellent cell viability when treated with $^{OH}Py_2N_2$. The levels of Nrf2 and downstream antioxidant enzyme GSH-dependent glutaredoxins (Grx1 and Grx2), important components that protect protein thiols from oxidation, increased ATP expression, and antiferroptotic potential were then measured to elucidate the catalytic protective mechanisms initiated by $^{OH}Py_2N_2$ treatment. Lastly, $^{OH}Py_2N_2$ was also found to prevent oxidative stress-induced lens opacity in an *ex vivo* organ culture model.

Materials and methods

General methods and materials

Ligand $^{OH}Py_2N_2$ was produced as the trihydrochloride salt using previously published methods (Johnston et al., 2019). Dulbecco's modified Eagle's medium (DMEM), fetal bovine serum (FBS), gentamicin, penicillin, and 0.05% trypsin were all purchased from Thermo Fisher Scientific (Waltham, MA, United States). Hydrogen peroxide and all chemicals were obtained from Sigma Chemical Co. (St. Louis, MO, United States) unless otherwise stated. Antibodies against Grx1 (ab45953) and Grx2 (ab45953) were purchased from Abcam (Waltham, MA, United States). Nrf2 (#12721) and GPX4 (#52455) antibodies were purchased from Cell Signaling (Denver, CO, United States). CellROX Deep Red was purchased from Thermo Fisher Scientific (Waltham, MA, United States). Colorimetric cell viability kit I (WST-8) was purchased from PromoKine (Heidelberg, Baden-Württemberg, Germany).

Potentiometric methods

The concentration of the $^{OH}Py_2N_2$ ligand, as well as an estimation of the stability constant of the iron (II) complex, were determined *via* pH-potentiometric titrations. Challenges with solubility prevented a high level of accuracy in the models. A Metrohm 888 Titrando equipped with a Metrohm 6.0234.100 combined electrode was used to measure the pH in the titration experiments. For the calibration of the electrode, KH-phthalate (pH 4.008) and borax (pH 9.177) buffers were used (Manov et al., 1945; Manov et al., 1946). The calculation of $[H^+]$ from the measured pH values was performed with the use of the method proposed by Irving *et al.* by titrating a 0.02 M HCl solution with a standardized NaOH solution (0.2 M) (Irving et al., 1967). The differences between the measured and calculated pH values were used to obtain the $[H^+]$ concentrations from the pH-data collected in the titrations. The ion product of water was determined from the same experiment in the pH range 11.40–12.00. The ionic strength in the titrated and thermostat controlled (at 25°C) samples of 6.00 ml was kept constant and set to 0.15 M NaCl. The samples were stirred by a magnetic stir bar and kept under inert gas atmosphere (N_2) to avoid the effect of CO_2. The protonation constants of the ligands were obtained from previously reported data (Johnston et al., 2019). Validation of the formation of the metal complex was determined using the direct pH-potentiometric method by titrating samples with 1:1 metal-to-ligand ratios (the number of data pairs were between 100 and

250), allowing 1 min for sample equilibration to occur. Models of the formation were obtained from the titration data with the PSEQUAD program (Bush, 2011). The protonation and metal complex stability pH titration were plotted against the first derivative of the slope to emphasis the formation of the iron (II) complex of the $^{OH}Py_2N_2$.

Primary mouse lens epithelial cell (LEC) culture

Primary LEC cultures were isolated from C57BL/6J mice. Mouse lens capsules were cut into small pieces and treated with 0.05% trypsin at 37°C for 10–20 min. The cells loosened from the capsule were placed into a 24-well plate containing 1 ml DMEM with 20% FBS and 50 μg/ml gentamicin per well. The cultures were incubated for 1 week in a humid atmosphere with 5% CO_2 at 37°C. Medium was changed every 2 days. After the primary cultures achieved confluence, the cells were subcultured by using 0.05% trypsin.

Lens organ culture

All experiments using mice were in accordance with the ARVO Statement for the Use of Animals in Ophthalmic and Vision Research and an approved institutional animal care and use committee protocol at the University of North Texas Health Science Center (Protocol Number: IACUC-2019-0003 and IACUC-2022-0008). The mouse lenses from C57BL/6J mice were carefully dissected out of the eye using a posterior approach to avoid the surgical tools damaging the lens. The lenses were cultured in modified TC-199 media by following previously published method (Cui and Lou, 1993). Briefly, the lenses were placed in a 24-well plate of TC-199 media with an osmolarity ranging from 300–320 mOsm. The medium was pre-incubated in an organ culture incubator at 37°C with 5% CO_2 for 2 h prior to the addition of the lenses. The lenses were then incubated in the medium for 24 h. Those lenses became opaque, an indication of potential damage due to dissection, were excluded from the following experiments. Cultured lenses were incubated with 10–100 μL $^{OH}Py_2N_2$ for 24 h and then exposed to 200 μm H_2O_2 for another 6 h. The lens morphological changes were recorded under a dissecting microscope (Nikon) using darkfield illuminations. Lenses incubated with media alone served as the control.

Cell viability assay

Cell viability was measured by a colorimetric cell viability kit (Promokine, Heidelberg, Germany) with the tetrazolium salt WST-8 (2-(2-methoxy-4-nitrophenyl)-3-(4-nitrophenyl)-5-(2,4-disulfophenyl)-2H-tetrazolium, monosodium salt), which can be bioreduced to a water-soluble orange formazan dye by dehydrogenases present in the viable cells. The amount of formazan produced is directly proportional to the number of living cells. Cells were seeded at a density of 5000 cells/well (100 μL total volume/well) in a 96-well assay. Cells were incubated with or without $^{OH}Py_2N_2$ (10 and 100 μm) for 24 h and then treated with 200 μm of H_2O_2 for 6 h. After treatment, 10 μL of WST-8 solution was added to each well of the culture plate and incubated for 2 h in the incubator. The absorption was evaluated at 450 nm using a microplate reader (BioTek, Winooski, VT). The cell morphology was observed under phase-contrast microscopy.

Cellular ROS assay

Intracellular ROS levels were determined using the fluorescent probe CellROX Orange Reagent. After pretreatment with $^{OH}Py_2N_2$ for 24 h, LECs were exposed to 200 μm H_2O_2 for another 30 min. After treatment, the cells were loaded with 5 mm CellROX Orange Reagent for 30 min at 37°C, washed with DPBS and immediately imaged on a fluorescence microscope (Olympus, Center Valley, PA). The cellular fluorescence was quantified using the ImageJ software, after background subtraction for each image.

Western blot analysis

Protein concentration was determined with a BCA assay kit (Thermo Scientific, Rockford, IL). Equal amounts of protein were boiled in Laemmli buffer (Bio-Rad, Bio-Rad, Richmond, CA, United States) and loaded onto 12% SDS-PAGE gel and transferred to a 0.2 μm polyvinylidene difluoride membrane (GE Healthcare, Boulder, CO). The membranes were incubated with appropriate primary antibodies for overnight at 4°C and were then incubated with the appropriate secondary antibodies for 1 h. Detection was performed using the ECL Western blotting detection system (Thermo Scientific, Rockford, IL). The immunoblot was analyzed with a Bio-Rad imaging system (Versadoc 5000 MP Imaging System, Bio-Rad, Richmond, CA, United States).

Glutaredoxin activity

The enzyme activities of Grx1 and Grx2 were examined using 2-Hydroxyethyl disulfide (HEDS) as the substrate according to the method described in Raghavachari and Lou (Gladyshev et al., 2001). In brief, the cell lysate was mixed with potassium phosphate buffer (200 mm, pH7.5) containing 0.5 mm glutathione (GSH), 0.4 U/mL glutathione reductase (GR),

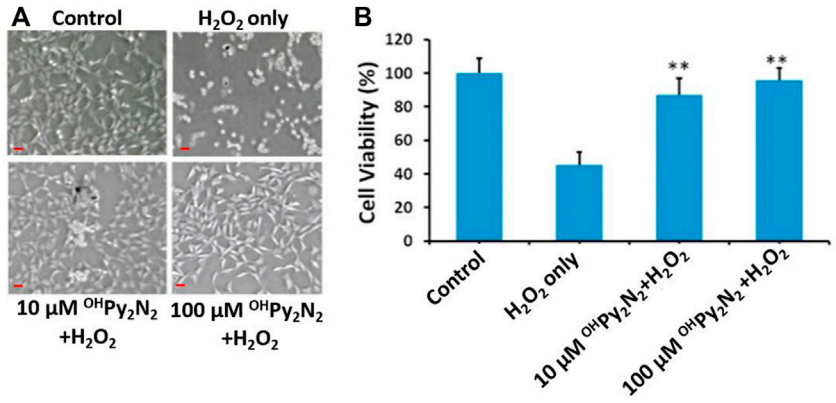

FIGURE 2
Cytoprotective effects of $^{OH}Py_2N_2$ in primary LEC against treatment with H_2O_2. Cells were incubated with or without $^{OH}Py_2N_2$ (10 and 100 μM) for 24 h and then treated with 200 μM of H_2O_2 for 6 h. After treatment, 10 μL of WST-8 solution was added to each well of the culture plate and incubated for 2 h in the incubator. **(A)** Images of cells (Scale bar = 50 μm), **(B)** Cell viability. n = 6, $^{**}p < 0.01$.

0.2 mm β-nicotinamide adenine dinucleotide phosphate, reduced tetra (cyclohexylammonium) salt (NADPH), and 2 mm hydroxyethyl disulfide (HED). The reaction was carried out at 30°C, and the decrease in absorbance at 340 nm was monitored for 5 min and used to determine the activity.

ATP Quantification

ATP level was measured with an ATP bioluminescence assay kit CLS II (Roche Applied Science, Penzberg, Germany) according to the manufacturer's recommendation (Wu et al., 2014). Briefly, lens homogenates were mixed with nine volumes of boiling solution (PBS containing 100 mm Tris and 4 mm EDTA) and incubated for 2 min at 100°C. The sample mix was then centrifuged at 1000 × g for 1 min, and 50 μL of the supernatant was mixed with 50 μL of luciferase reagent by automated injection. The luminescence intensity was detected by a Fluostar Optima microplate reader (BMG Labtech, Offenburg, Germany), and integrated for 1–10 s.

Malondialdehyde (MDA) measurement

Cells were seeded at a density of 10,000 cells/well in a 96-well assay. Cells were incubated with or without $^{OH}Py_2N_2$ (1, 10 and 100 μm) for 24 h and then treated with 200 μm of H_2O_2 for 6 h. MDA was measured by using the MDA assay kit (Abcam, Cambridge, MA, United States, ab118970) based on the thiobarbituric acid (TBA) reaction. The intensity of the resulting MDA-TBA adduct was read at RFU at Ex/Em = 532/553 nm and the data were expressed as nmol/mg protein.

Statistics

Each experiment was performed at least three times and statistical analyses were performed using Student's t-test when comparing between two groups and one-way ANOVA followed by Bonferroni's test as a post hoc test when comparing among three or more groups with the Prism software (GraphPad, La Jolla, CA). The number of experimental samples used in each group is presented in the figure legends. All data are expressed as means ± SD and differences were considered significant at $p < 0.05$.

Results and discussion

Previous work has shown that pyridinophane type molecules are low molecular weight entities that display potent antioxidant ability, low toxicity, and high metabolic stability in neuronal cell culture models, suggesting they could serve as potential agents to treat Alzheimer's and other neurodegenerative diseases (Lincoln et al., 2013; Green et al., 2019; Johnston et al., 2019). Among these molecules, the $^{OH}Py_2N_2$ pyridinophane (Figure 1) showed higher pharmacological efficacy and increased biological compatibility compared to the parent systems (Johnston et al., 2019). As a result of this success, disorders of the eye were next explored to understand the extent to which the protective nature of $^{OH}Py_2N_2$ could be utilized and as models to understand the mechanisms of this protective reactivity.

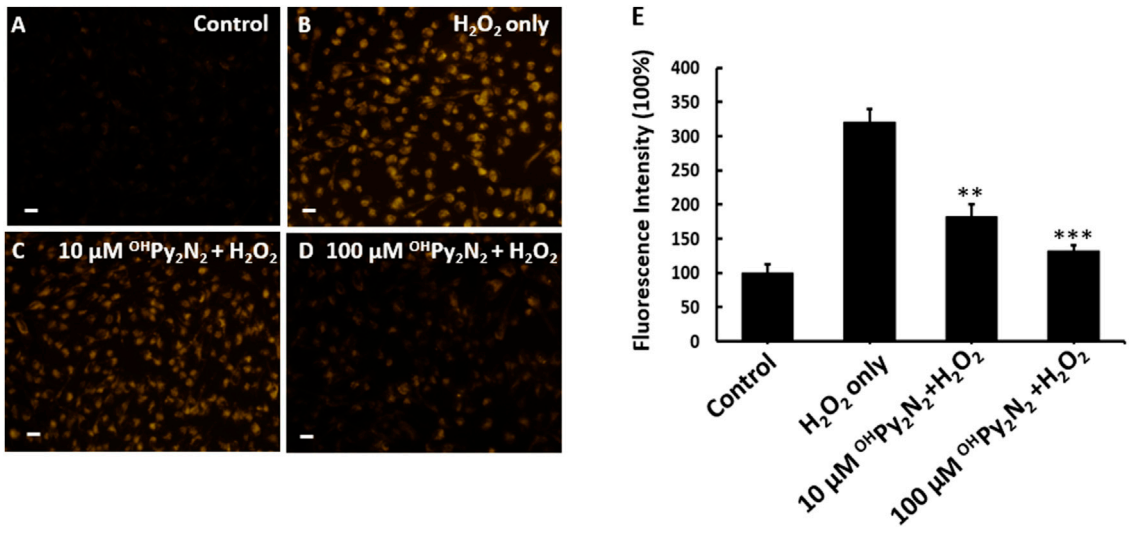

FIGURE 3
$^{OH}Py_2N_2$ reduces ROS production in H_2O_2-treated LECs. **(A)** LECs as a control with no treatment, **(B)** 200 μM H_2O_2 treatment for 30 min, and **(C,D)** pretreatment with 10 or 100 μM $^{OH}Py_2N_2$ for 24 h followed by 200 μM H_2O_2 treatment for 30 min. **(E)** Fluorescence was detected using the probe CellROX orange reagent for all groups; fluorescence intensity quantified and represented as the mean mean ± SEM of three independent experiments, $^{**}p < 0.01$, $^{***}p < 0.01$ compared with the H_2O_2-only group ($n = 3$). Scale bar = 50 μm.

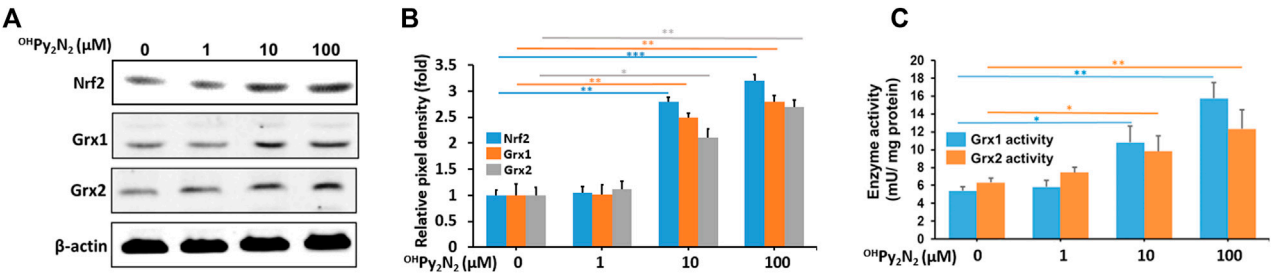

FIGURE 4
$^{OH}Py_2N_2$ upregulates Nrf2, Grx1, and Grx2 in LECs.**(A)** Western blot analysis showing the increased expression of antioxidant transcription factor Nrf2 along with enzymes Grx1, and Grx2. **(B)** The relative pixel density of Nrf2, Grx1, and Grx2 over loading control. **(C)** Grx1 and Grx2 enzymatic activity increased as a result of exposure to $^{OH}Py_2N_2$. ($^{*}p < 0.05$; $^{**}p < 0.01$; $^{***}p < 0.001$) ($n = 3$).

$^{OH}Py_2N_2$ prevents LECs from H_2O_2-induced damage

To test the cytoprotective effects in the lens, primary LECs were treated with $^{OH}Py_2N_2$ for 24 h followed by a 200 μm H_2O_2 challenge for 6 h H_2O_2 treatment alone caused approximately 60% cell viability loss in mLECs (Figure 2). In contrast, treatments of $^{OH}Py_2N_2$ at concentrations of both 10 μm and 100 μm $^{OH}Py_2N_2$ protected cells from oxidative stress-induced cell damage, with the later showing the largest (90%) improvement. The cell morphology was then observed under phase-contrast microscopy. Following exposure to 200 μm H_2O_2 for 6 h, LECs showed a marked decrease in number concomitant to shrinkage in size and loss of adhesion. Pretreatment with different doses of $^{OH}Py_2N_2$ (10 and 100 μm) attenuated H_2O_2-induced cell morphological changes. These results suggest that the $^{OH}Py_2N_2$ molecule can prevent cell death induced by oxidative stress in multiple models, making its translation to multiple disease states arising from oxidative stress promising.

$^{OH}Py_2N_2$ prevents ROS production

Intracellular ROS levels were measured to determine if the protection demonstrated by $^{OH}Py_2N_2$ against H_2O_2 (Figure 2) induced cell death as a result of lowering the oxidative stress in the LECs. For this study, cells were preloaded with CellROX Orange followed by stimulation with H_2O_2 to monitor the resulting ROS sensitive fluorescent product (Figure 3). Separately, LECs were pretreated with $^{OH}Py_2N_2$ for 24 h and subsequently treated with H_2O_2 at 200 μm for another 30 min. As compared with non-treated control cells (Figure 3A), H_2O_2 treatment significantly increased the fluorescence intensity of ROS (Figure 3B). $^{OH}Py_2N_2$ treatment dose-dependently decreased the production of ROS (Figures 3C,D). Quantitative fluorescence intensities of CellROX Orange in the various groups are shown in Figure 3E to support the visual results and validate that the $^{OH}Py_2N_2$ molecule protects against ROS induced cell death by H_2O_2 by decreasing the oxidative stress in the LECs.

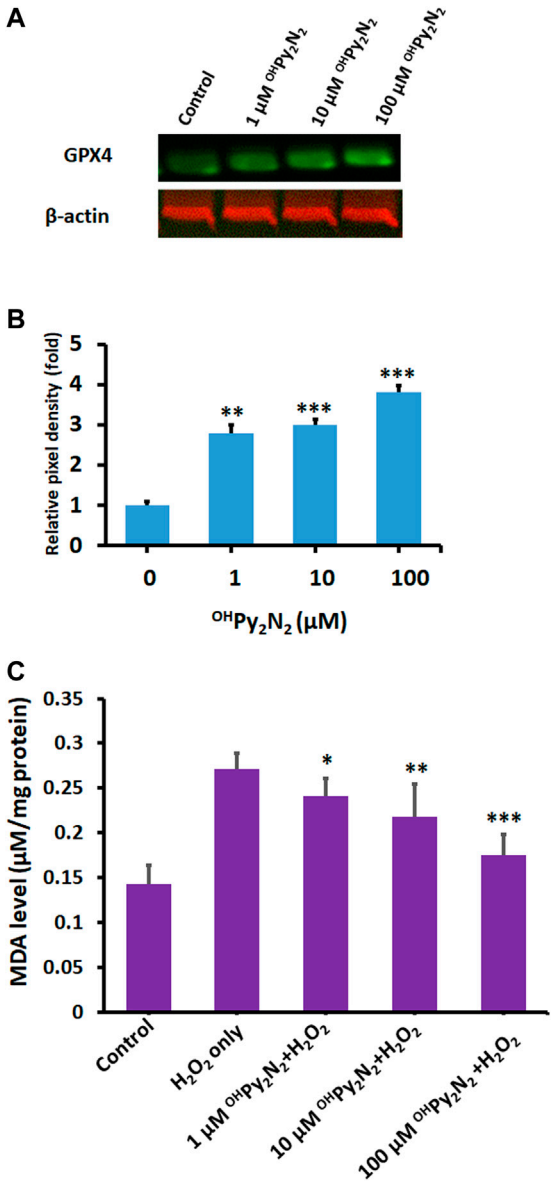

FIGURE 5
Anti-ferroptotic effects of $^{OH}Py_2N_2$ in LECs. **(A)** $^{OH}Py_2N_2$ upregulates GPX4 expression. LECs were treated with (1–100 μM) $^{OH}Py_2N_2$ for 24 h. Control cells were treated identically but without additional of $^{OH}Py_2N_2$. **(B)** The relative pixel density of GPX4 over loading control. Data presented are a typical representation of triplicate experiments. (**$p < 0.01$; ***$p < 0.001$). **(C)** $^{OH}Py_2N_2$ inhibits H_2O_2-induced MDA formation. Cells were incubated with or without $^{OH}Py_2N_2$ (1, 10 and 100 μM) for 24 h and then treated with 200 μm of H_2O_2 for 6 h. MDA level in each group was measured. (*$p < 0.05$; **$p < 0.01$; ***$p < 0.001$) ($n = 3$).

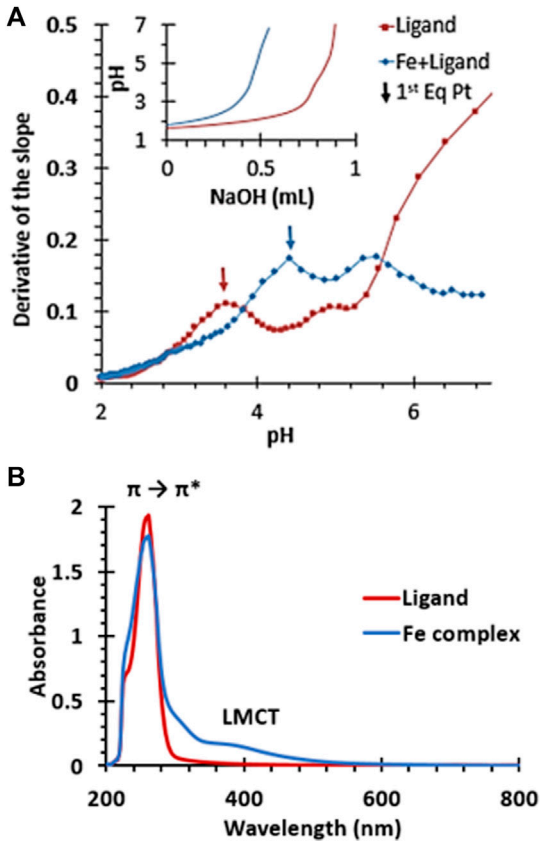

FIGURE 6
(A) First derivative of the potentiometric titration of $^{OH}Py_2N_2$ and the iron (II) complex. Inset shows original titration data. **(B)** UV-vis spectra of an aqueous solution of $^{OH}Py_2N_2$ (red) and **(B)** the iron (III) complex of $^{OH}Py_2N_2$.

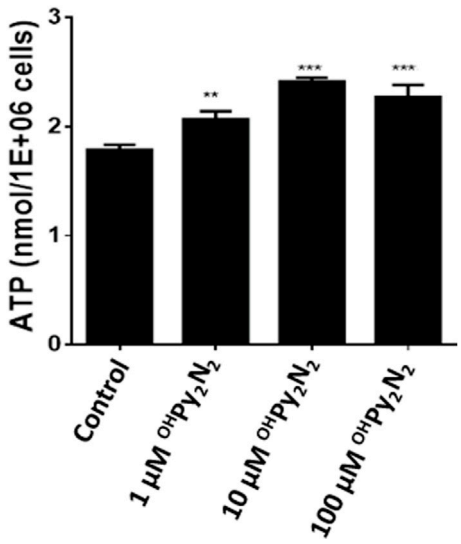

FIGURE 7
ATP production is increased with the addition of $^{OH}Py_2N_2$. LECs were treated with (1–100 μm) $^{OH}Py_2N_2$ for 24 h. Control cells were treated identically but without additional of $^{OH}Py_2N_2$. Whole cell homogenates were used for ATP measurement with an ATP assay kit (n = 6, $^{**}p < 0.01$, $^{***}p < 0.001$).

$^{OH}Py_2N_2$ activates Nrf2 and increases glutaredoxin (Grx) expression

Nrf2 is the central regulator of a comprehensive and protective biological antioxidant response. Activation of Nrf2 leads to the transcriptional activation of a broad range of antioxidant enzymes including NADPH dehydrogenase, heme oxygenase-1, superoxide dismutase, catalase, glutathione peroxidase (GPX), thioredoxin, and more. Our previous study has shown that $^{OH}Py_2N_2$ could dose-dependently upregulate Nrf2 in neuronal cell culture (Johnston et al., 2019). Therefore, LECs were treated with $^{OH}Py_2N_2$ at 1, 10, and 100 μm for 24 h to further investigate the effect on the Nrf2 pathway in this particular model. Western blot analysis showed a dose-dependent increase of Nrf2 protein expression (Figure 4A). This result indicates that the mode of antioxidant action (Nrf2 expression) is translated between neuronal and lens cell culture showing the portability of this molecule toward treating conditions rising from oxidative stress. As a result of this success, we next explored what mechanisms could be activated as a result of Nrf2 expression upon treatment with $^{OH}Py_2N_2$ resulting in the protective effects observed to date.

To maintain intracellular redox homeostasis, mammalian tissues including the lens have well-designed repair systems to protect protein thiols from oxidation (Holmgren, 1989; Lillig et al., 2008). The first is the GSH-dependent glutaredoxin (Grx) system, which are a group oxidoreductases that catalyze the reduction of glutathione-protein mixed disulfides. The Grx system has two major isozymes: glutaredoxin 1 (Grx1, also known as thioltransferase or TTase) and the recently discovered glutaredoxin 2 (Grx2) (Holmgren, 1976; Gladyshev et al., 2001; Lundberg et al., 2001). Previous studies suggest that enhancing Grx system may be a potential therapeutic strategy for delaying or slowing down the age-related cataracts (Xing and Lou, 2010; Kronschläger et al., 2012; Wu et al., 2014; Fan et al., 2022). In our study, we found $^{OH}Py_2N_2$ could boost activity of the Grx system. The enzymatic activity of Grx1 and Grx2 were observed to increase in cell lysates treated with $^{OH}Py_2N_2$ (1–100 μm) in a dose-dependently manner (Figure 4B) along with the protein levels of Grx1 and Grx2 (Figure 4A). From this series of studies, it can be concluded that the addition of $^{OH}Py_2N_2$ to LECs activates the translocation of Nrf2 and the expression of antioxidant enzymes, including Grx1 and Grx2 as a mechanism that results in the catalytic protection of LECs against ROS assaults. To our knowledge this is the first example of a such a low molecular weight, macrocyclic small molecule of this type,

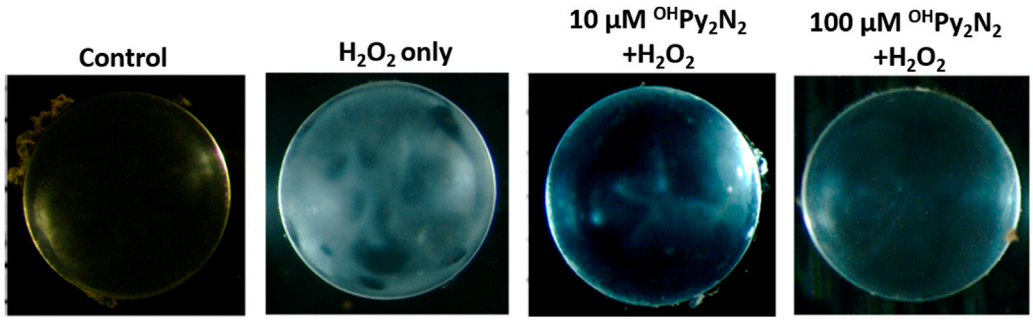

FIGURE 8
$^{OH}Py_2N_2$ prevented H_2O_2-induced opacity in culture mouse lenses. Cultured lenses were incubated with 10–100 μm $^{OH}Py_2N_2$ for 24 h and then exposed to 200 μm H_2O_2 for another 6 h (n = 3).

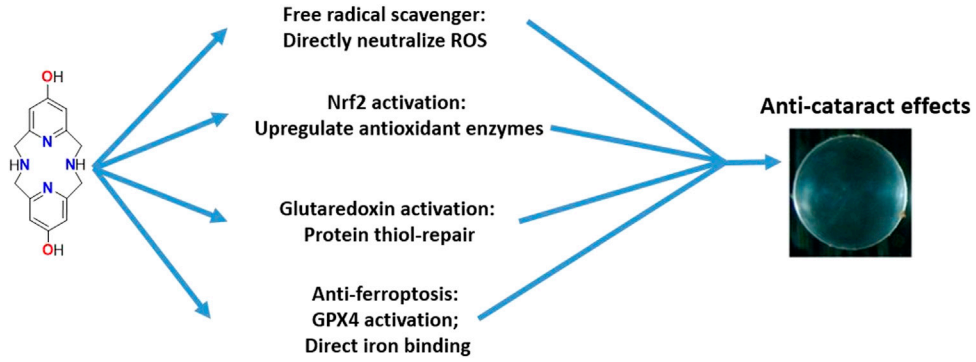

FIGURE 9
Multiple pathways are activated upon exposure to $^{OH}Py_2N_2$ that can result in protection against oxidative stress and cataract formation.

particularly a pyridinophane, that can activate cellular mechanisms of protection against oxidative stress.

$^{OH}Py_2N_2$ demonstrates anti-ferroptotic effects and iron binding

Ferroptosis is a newly identified form of non-apoptotic regulated cell death that is initiated by excessive iron-dependent lipid peroxidation (Jiang et al., 2021). Glutathione peroxidase (GPX4) is the key regulator of this form of cell death (Lei et al., 2022). Compounds that up-regulate GPX4 have been proposed as ferroptosis inhibitors (Chen et al., 2020; Li et al., 2020; Lei et al., 2022). In fact, inhibiting ferroptosis has the potential to be a useful therapeutic method for age-related diseases, including cataract (Wei et al., 2021). In our study, we found $^{OH}Py_2N_2$ dose-dependently upregulate GPX4 in LECs (Figures 5A,B), indicating $^{OH}Py_2N_2$, thus enhancing a natural defense mechanism against ferroptosis.

Ferroptosis is associated with two major biochemical hallmarks, lipid peroxidation and iron accumulation (Tang et al., 2021). Malondialdehyde (MDA), the final product of polyunsaturated fatty acid peroxidation, is one of the most important biomarkers of lipid peroxidation. Previous studies have shown that MDA accumulation plays a pivotal role in senile cataractogenesis (Bhuyan et al., 1986). As shown in Figure 5C, as compared with the control group, the MDA level was significantly increased after H_2O_2 treatment (control: 0.14 ± 0.021 vs. H_2O_2 alone: 0.27 ± 0.0172 nmol/mg protein, $p <$ 0.001). Conversely, $^{OH}Py_2N_2$ prevented H_2O_2-induced MDA accumulation in a dose-dependent manner (1 μM $^{OH}Py_2N_2$: 0.24 ± 0.022 nmol/mg protein $p < 0.05$ vs. 10 μm $^{OH}Py_2N_2$: 0.21 ± 0.035 nmol/mg protein $p < 0.01$ vs. 100 μM $^{OH}Py_2N_2$: 0.17 ± 0.023 nmol/mg protein $p < 0.001$). Our data indicate that $^{OH}Py_2N_2$ effectively prevented oxidative stress-induced lipid peroxidation.

Additionally, iron-chelating capacity is also strongly linked with anti-ferroptotic effects (Chen et al., 2020; Lei et al., 2022).

The metal binding halts the Fenton reaction that leads to ferroptotic lipid peroxidation. Molecule $^{OH}Py_2N_2$ has previously been shown to bind copper (II) effectively and molecules within this pyridinophane family are well-known to interact strongly with a range of transition metal-ions including iron (II) and (III) (Brewer et al., 2018; Johnston et al., 2019; Mekhail et al., 2020; Brewer et al., 2021). Potentiometric titrations of $^{OH}Py_2N_2$ and iron (II) in aqueous solution (Figure 6) validate complexation based on the shift in the titration curve compared to the chelate molecule alone. This curve is very similar to our previous studies of similar iron (II) titrations showing complex formation around a pH of four and is consistent with a log β in the range of 12–13, which is in range or higher than metal-binding agents explored to date (Chen et al., 2020; Mekhail et al., 2020). Furthermore, addition of iron (III) to an aqueous solution of $^{OH}Py_2N_2$ resulted in a color change from pale yellow to dark yellow. UV-vis analysis of the resulting solution showed ligand to metal charge transfer bands at 313 and 390 nm (Figure 6) and a ligand based π to π* transition at 290 nm. This spectroscopy is consistent with an Fe(III) ($^{OH}Py_2N_2$)Cl_2 complex of the geometry shown in Figure 1 (Mekhail et al., 2020; Brewer et al., 2021). Together, these results serve as evidence that the $^{OH}Py_2N_2$ scaffold is a good agent for binding iron (II) and (III) and could be a contributing mechanism for antiferroptotic activity to explore in depth in the future.

$^{OH}Py_2N_2$ treatment promotes ATP production

Adenosine triphosphate (ATP) is often referred to as the "energy currency" because it is used to fill any energy needs of the cell. Reduced energy levels threaten cellular homeostasis and may trigger cataract formation (Greiner and Glonek, 2020). As a result of these foundations, the ability for $^{OH}Py_2N_2$ to elevate ATP production as a means of preventing oxidative stress induced cataract formation was explored using an established luciferase based bioluminescence assay method (Wu et al., 2014). The $^{OH}Py_2N_2$ molecule promoted a dose-dependently ATP production, suggesting that $^{OH}Py_2N_2$ may enhance mitochondrial function and improve bioenergetic function to help LECs to fight against oxidative stress (Figure 7).

$^{OH}Py_2N_2$ protects the lens from H_2O_2-induced opacity

Encouraged by the above positive results, we further tested if $^{OH}Py_2N_2$ treatments could prevent H_2O_2-induced lens opacity. Cultured lenses extracted from C57BL/6J mice were incubated with $^{OH}Py_2N_2$ (10–100 μm) for 24 h and then exposed to 200 μm H_2O_2 for another 6 h. As shown in Figure 8, pretreatment with 10 and 100 μm $^{OH}Py_2N_2$, followed by H_2O_2 induction, resulted in reduced opacities compared to cataract induction alone.

Conclusion

The studies show that the ability for $^{OH}Py_2N_2$ to induce protection against peroxide induced cell death over to LECs (Figure 9). Although $^{OH}Py_2N_2$ was designed to serve as a direct antioxidant that functions through radical scavenging and metal-binding, the studies described herein show that the molecule activates multiple biological pathways innate to cells that promote the cells to protect against oxidative stress. The ability for $^{OH}Py_2N_2$ to turn-on Nrf2 expression as well as Grx1 and Grx2 catalytic pathways impacted by the small molecule. The molecule also upregulates GPX4 and binds iron (II) and (III) ions, which suggests that it should be explored further for the details regarding its anti-ferroptotic abilities in more detail. The bioenergetic pathway is also upregulated by treatment with $^{OH}Py_2N_2$ as evidenced by increased levels of ATP. Lastly, cultured lenses were protected from H_2O_2-induced lens opacity by this multimodal small molecule, showing the ultimate potential of this water-soluble small molecule. Altogether, this work opens up several new fields of exploration that marry the organic and inorganic design of small molecules with studies that function to elucidate an understanding of their potential to impact diseases in the eye. Moreover, understanding what structural components of the $^{OH}Py_2N_2$ molecule are responsible for activating these pathways is of urgent interest. This work also leads to the need to understand at what point(s) in the immune response pathway for protecting against oxidative stress the $^{OH}Py_2N_2$ interacts, leading to the responses described herein.

Data availability statement

The original contributions presented in the study are included in the article, further inquiries can be directed to the corresponding authors.

Author contributions

The manuscript was written through contributions of all authors. All authors have given approval to the final version of the manuscript.

Funding

The authors acknowledge National Institutes of Health 2R15GM123463-02 (to KG and HW) and Welch Foundation P-2063-20210327 (to KG). BrightFocus Foundation [rant no: M2015180 (HW)]; California Table Grape Commission

Research Grant (HW); and the United States Department of Defense [VRP Research Award no: W81XWH2010896 (HW)].

Conflict of interest

The authors declare that the research was conducted in the absence of any commercial or financial relationships that could be construed as a potential conflict of interest.

Publisher's note

All claims expressed in this article are solely those of the authors and do not necessarily represent those of their affiliated organizations, or those of the publisher, the editors and the reviewers. Any product that may be evaluated in this article, or claim that may be made by its manufacturer, is not guaranteed or endorsed by the publisher.

References

Age-Related Eye Disease Study Research Group (2001). A randomized, placebo-controlled, clinical trial of high-dose supplementation with vitamins C and E, beta carotene, and zinc for age-related macular degeneration and vision loss: AREDS report no. 8. *Arch. Ophthalmol.* 119 (10), 1417–1436. doi:10.1001/archopht.119.10.1417

Alzheimer's Disease Facts (2016). Figures, Alzheimer's & dementia. *Alzheimer's Assoc.* 12 (4).

Bahn, G., Park, J.-S., Yun, U. J., Lee, Y. J., Choi, Y., Park, J. S., et al. (2019). NRF2/ARE pathway negatively regulates BACE1 expression and ameliorates cognitive deficits in mouse Alzheimer's models. *Proc. Natl. Acad. Sci. U. S. A.* 116 (25), 12516–12523. doi:10.1073/pnas.1819541116

Beatty, S., Koh, H.-H., Phil, M., Henson, D., and Boulton, M. (2000). The role of oxidative stress in the pathogenesis of age-related macular degeneration. *Surv. Ophthalmol.* 45 (2), 115–134. doi:10.1016/s0039-6257(00)00140-5

Bhuyan, K. C., Bhuyan, D. K., and Podos, S. M. (1986). Lipid peroxidation in cataract of the human. *Life Sci.* 38 (16), 1463–1471. doi:10.1016/0024-3205(86)90559-x

Bosco, J. L. F., Antonsen, S., Sorensen, H. T., Pedersen, L., and Lash, T. L. (2011). Metformin and incident breast cancer among diabetic women: A population-based case-control study in Denmark. *Cancer Epidemiol. Biomarkers Prev.* 20 (1), 101–111. doi:10.1158/1055-9965.epi-10-0817

Brewer, S. M., Schwartz, T. M., Mekhail, M. A., Turan, L. S., Prior, T. J., Hubin, T. J., et al. (2021). Mechanistic insights into iron-catalyzed C–H bond activation and C–C coupling. *Organometallics* 40 (15), 2467–2477. doi:10.1021/acs.organomet.1c00211

Brewer, S. M., Wilson, K. R., Jones, D. G., Reinheimer, E. W., Archibald, S. J., Prior, T. J., et al. (2018). Increase of direct C–C coupling reaction yield by identifying structural and electronic properties of high-spin iron tetra-azamacrocyclic complexes. *Inorg. Chem.* 57 (15), 8890–8902. doi:10.1021/acs.inorgchem.8b00777

Bush, A. I. (2011). A copper binding site within the pathological conformer epitope of mutant SOD1. *Front. Neurosci.* 2, 97. doi:10.3389/fnins.2011.00097

Chan, E., Mahroo, O. A., and Spalton, D. J. (2010). Complications of cataract surgery. *Clin. Exp. Optom.* 93 (6), 379–389. doi:10.1111/j.1444-0938.2010.00516.x

Chen, X., Yu, C., Kang, R., and Tang, D. (2020). Iron metabolism in ferroptosis. *Front. Cell Dev. Biol.* 8, 590226. doi:10.3389/fcell.2020.590226

Chew, E. Y., Clemons, T. E., Agrón, E., Sperduto, R. D., SanGiovanni, J. P., Kurinij, N., et al. (2013). Long-term effects of vitamins C and E, β-carotene, and zinc on age-related macular degeneration: AREDS report no. 35. *Ophthalmology* 120 (8), 1604–1611.e4. e4. doi:10.1016/j.ophtha.2013.01.021

Cooper, G., Young, A., Gamble, G., Occleshaw, C., Dissanayake, A., Cowan, B., et al. (2009). A copper (II)-selective chelator ameliorates left-ventricular hypertrophy in type 2 diabetic patients: A randomised placebo-controlled study. *Diabetologia* 52 (4), 715–722. doi:10.1007/s00125-009-1265-3

Crielaard, B. J., Lammers, T., and Rivella, S. (2017). Targeting iron metabolism in drug discovery and delivery. *Nat. Rev. Drug Discov.* 16 (6), 400–423. doi:10.1038/nrd.2016.248

Cuadrado, A., Kügler, S., and Lastres-Becker, I. (2018). Pharmacological targeting of GSK-3 and NRF2 provides neuroprotection in a preclinical model of tauopathy. *Redox Biol.* 14, 522–534. doi:10.1016/j.redox.2017.10.010

Cui, X.-L., and Lou, M. F. (1993). The effect and recovery of long-term H2O2 exposure on lens morphology and biochemistry. *Exp. eye Res.* 57 (2), 157–167. doi:10.1006/exer.1993.1111

Czerska, M., Mikolajewska, K., Zielinski, M., Gromadzinska, J., and Wasowicz, W. (2015). Today's oxidative stress markers. *Med. Pr.* 66 (3), 393–405. doi:10.13075/mp.5893.00137

D'Souza, L. C., Mishra, S., Chakraborty, A., Shekher, A., Sharma, A., and Gupta, S. C. (2020). Oxidative stress and cancer development: Are noncoding RNAs the missing links? *Antioxidants Redox Signal.*

DeCensi, A., Puntoni, M., Goodwin, P., Cazzaniga, M., Gennari, A., Bonanni, B., et al. (2010). Metformin and cancer risk in diabetic patients: A systematic review and meta-analysis. *Cancer Prev. Res. (Phila).* 3 (11), 1451–1461. doi:10.1158/1940-6207.capr-10-0157

Doig, A. J., Del Castillo-Frias, M. P., Berthoumieu, O., Tarus, B., Nasica-Labouze, J., Sterpone, F., et al. (2017). Why is research on amyloid-beta failing to give new drugs for alzheimer's disease? *ACS Chem. Neurosci.* 8 (7), 1435–1437. doi:10.1021/acschemneuro.7b00188

Fan, Q., Li, D., Zhao, Z., Jiang, Y., and Lu, Y. (2022). Protective effect of Glutaredoxin 1 against oxidative stress in lens epithelial cells of age-related nuclear cataracts. *Mol. Vis.* 28, 70–82.

Farrawell, N. E., Yerbury, M. R., Plotkin, S. S., McAlary, L., and Yerbury, J. J. (2018). CuATSM protects against the *in vitro* cytotoxicity of wild-type-like copper–zinc superoxide dismutase mutants but not mutants that disrupt metal binding. *ACS Chem. Neurosci.* 10 (3), 1555–1564. doi:10.1021/acschemneuro.8b00527

Fraser, G. E. (2009). Vegetarian diets: What do we know of their effects on common chronic diseases? *Am. J. Clin. Nutr.* 89 (5), S1607–S1612. doi:10.3945/ajcn.2009.26736k

Giem, P., Beeson, W. L., and Fraser, G. E. (1993). The incidence of dementia and intake of animal products - preliminary findings from the adventist health study. *Neuroepidemiology* 12 (1), 28–36. doi:10.1159/000110296

Gladyshev, V. N., Liu, A., Novoselov, S. V., Krysan, K., Sun, Q. A., Kryukov, V. M., et al. (2001). Identification and characterization of a new mammalian glutaredoxin (thioltransferase), Grx2. *J. Biol. Chem.* 276 (32), 30374–30380. doi:10.1074/jbc.m100020200

Goodson, A. G., Cotter, M. A., Cassidy, P., Wade, M., Florell, S. R., Liu, T., et al. (2009). Use of oral N-acetylcysteine for protection of melanocytic nevi against UV-induced oxidative stress: Towards a novel paradigm for melanoma chemoprevention. *Clin. Cancer Res.* 15 (23), 7434–7440. doi:10.1158/1078-0432.ccr-09-1890

Green, K. N., Pota, K., Tircsó, G., Gogolák, R. A., Kinsinger, O., Davda, C., et al. (2019). Dialing in on pharmacological features for a therapeutic antioxidant small molecule. *Dalton Trans.* 48, 12430–12439. doi:10.1039/c9dt01800j

Greiner, J. V., and Glonek, T. (2020). Hydrotropic function of ATP in the crystalline lens. *Exp. Eye Res.* 190, 107862. doi:10.1016/j.exer.2019.107862

Han, Y., Nan, S., Fan, J., Chen, Q., and Zhang, Y. (2019). Inonotus obliquus polysaccharides protect against Alzheimer's disease by regulating Nrf2 signaling

and exerting antioxidative and antiapoptotic effects. *Int. J. Biol. Macromol.* 131, 769–778. doi:10.1016/j.ijbiomac.2019.03.033

Holmgren, A. (1976). Hydrogen donor system for *Escherichia coli* ribonucleoside-diphosphate reductase dependent upon glutathione. *Proc. Natl. Acad. Sci. U. S. A.* 73 (7), 2275–2279. doi:10.1073/pnas.73.7.2275

Holmgren, A. (1989). Thioredoxin and glutaredoxin systems. *J. Biol. Chem.* 264 (24), 13963–13966. doi:10.1016/s0021-9258(18)71625-6

Ikawa, M., Okazawa, H., Tsujikawa, T., Matsunaga, A., Yamamura, O., Mori, T., et al. (2015). Increased oxidative stress is related to disease severity in the ALS motor cortex: A PET study. *Neurology* 84 (20), 2033–2039. doi:10.1212/wnl.0000000000001588

Irving, H. M., Miles, M. G., and Pettit, L. D. (1967). A study of some problems in determining the stoicheiometric proton dissociation constants of complexes by potentiometric titrations using a glass electrode. *Anal. Chim. Acta* 38 (4), 475–488. doi:10.1016/s0003-2670(01)80616-4

Jarvis, L. M. (2015). Alzheimer's next chapter. *Chem. Eng. News Arch.* 93, 11–15. doi:10.1021/cen-09322-cover

Jiang, X., Stockwell, B. R., and Conrad, M. (2021). Ferroptosis: Mechanisms, biology and role in disease. *Nat. Rev. Mol. Cell Biol.* 22 (4), 266–282. doi:10.1038/s41580-020-00324-8

Johnson, J., Maher, P., and Hanneken, A. (2009). The flavonoid, eriodictyol, induces long-term protection in ARPE-19 cells through its effects on Nrf2 activation and phase 2 gene expression. *Invest. Ophthalmol. Vis. Sci.* 50 (5), 2398–2406. doi:10.1167/iovs.08-2088

Johnston, H. M., Pota, K., Barnett, M. M., Kinsinger, O., Braden, P., Schwartz, T. M., et al. (2019). Enhancement of the antioxidant activity and neurotherapeutic features through pyridol addition to tetraazamacrocyclic molecules. *Inorg. Chem.* 58 (24), 16771–16784. doi:10.1021/acs.inorgchem.9b02932

Kaspar, J. W., Niture, S. K., and Jaiswal, A. K. (2009). Nrf2:INrf2 (Keap1) signaling in oxidative stress. *Free Radic. Biol. Med.* 47 (9), 1304–1309. doi:10.1016/j.freeradbiomed.2009.07.035

Kingwell, K. (2017). Zeroing in on neurodegenerative alpha-synuclein. *Nat. Rev. Drug Discov.* 16 (6), 371–373. doi:10.1038/nrd.2017.95

Kitaoka, Y., Tamura, Y., Takahashi, K., Takeda, K., Takemasa, T., and Hatta, H. (2019). Effects of Nrf2 deficiency on mitochondrial oxidative stress in aged skeletal muscle. *Physiol. Rep.* 7 (3), e13998. doi:10.14814/phy2.13998

Kronschläger, M., Galichanin, K., Ekström, J., Lou, M. F., and Söderberg, P. G. (2012). Protective effect of the thioltransferase gene on *in vivo* UVR-300 nm–induced cataract. *Invest. Ophthalmol. Vis. Sci.* 53 (1), 248–252. doi:10.1167/iovs.11-8504

Lannfelt, L., Blennow, K., Zetterberg, H., Batsman, S., Ames, D., Harrison, J., et al. (2008). Safety, efficacy, and biomarker findings of PBT2 in targeting aβ as a modifying therapy for alzheimer's disease: A phase IIa, double-blind, randomised, placebo-controlled trial. *Lancet Neurol.* 7 (9), 779–786. doi:10.1016/s1474-4422(08)70167-4

Lei, G., Zhuang, L., and Gan, B. (2022). Targeting ferroptosis as a vulnerability in cancer. *Nat. Rev. Cancer* 22 (7), 381–396. doi:10.1038/s41568-022-00459-0

Li, J., Cao, F., Yinliang, H., Huangjian, Z., Lintao, Z., Mao, N., et al. (2020). Ferroptosis: Past, present and future. *Cell Death Dis.* 11 (2), 88. doi:10.1038/s41419-020-2298-2

Lillig, C. H., Berndt, C., and Holmgren, A. (2008). Glutaredoxin systems. *Biochimica Biophysica Acta - General Subj.* 1780 (11), 1304–1317. doi:10.1016/j.bbagen.2008.06.003

Lincoln, K. M., Gonzalez, P., Richardson, T. E., Rutter, L., Julovich, D. A., Simpkins, J. W., et al. (2013). A potent antioxidant small molecule aimed at targeting metal-based oxidative stress in neurodegenerative disorders. *Chem. Commun.* 49, 2712–2714. doi:10.1039/c2cc36808k

Lofgren, S. (2017). Solar ultraviolet radiation cataract. *Exp. Eye Res.* 156, 112–116. doi:10.1016/j.exer.2016.05.026

Lou, M. F. (2003). Redox regulation in the lens. *Prog. Retin. eye Res.* 22 (5), 657–682. doi:10.1016/s1350-9462(03)00050-8

Lundberg, M., Johansson, C., Chandra, J., Enoksson, M., Jacobsson, G., Ljung, J., et al. (2001). Cloning and expression of a novel human glutaredoxin (Grx2) with mitochondrial and nuclear isoforms. *J. Biol. Chem.* 276 (28), 26269–26275. doi:10.1074/jbc.m011605200

Ma, Q. (2013). Role of nrf2 in oxidative stress and toxicity. *Annu. Rev. Pharmacol. Toxicol.* 53, 401–426. doi:10.1146/annurev-pharmtox-011112-140320

Manov, G. G., Delollis, N. J., and Acree, S. F. (1945). Comparative liquid-junction potentials of some ph buffer standards and the calibration of ph meters. *J. Res. Natl. Bur. Stand. (1977).* 34 (2), 115–127. doi:10.6028/jres.034.002

Manov, G. G., Delollis, N. J., Lindvall, P. W., and Acree, S. F. (1946). Effect of sodium chloride on the apparent ionization constant of boric acid and the ph values of borate solutions. *J. Res. Natl. Bur. Stand. (1977).* 36 (6), 543–558. doi:10.6028/jres.036.033

Mekhail, M. A., Pota, K., Schwartz, T. M., and Green, K. N. (2020). Functionalized pyridine in pyclen-based iron (iii) complexes: Evaluation of fundamental properties. *RSC Adv.* 10 (52), 31165–31170. doi:10.1039/d0ra05756h

Naik, P., Fofaria, N., Prasad, S., Sajja, R. K., Weksler, B., Couraud, P. O., et al. (2014). Oxidative and pro-inflammatory impact of regular and denicotinized cigarettes on blood brain barrier endothelial cells: Is smoking reduced or nicotine-free products really safe? *BMC Neurosci.* 15, 51. doi:10.1186/1471-2202-15-51

Nechuta, S., Lu, W., Chen, Z., Zheng, Y., Gu, K., Cai, H., et al. (2011). Vitamin supplement use during breast cancer treatment and survival: A prospective cohort study. *Cancer Epidemiol. Biomarkers Prev.* 20 (2), 262–271. doi:10.1158/1055-9965.epi-10-1072

Niedzielska, E., Smaga, I., Gawlik, M., Moniczewski, A., Stankowicz, P., Pera, J., et al. (2016). Oxidative stress in neurodegenerative diseases. *Mol. Neurobiol.* 53 (6), 4094–4125. doi:10.1007/s12035-015-9337-5

Organization, W. H. (2019). *World report on vision*.

Patel, M. (2016). Targeting oxidative stress in central nervous system disorders. *Trends Pharmacol. Sci.* 37 (9), 768–778. doi:10.1016/j.tips.2016.06.007

Pisoschi, A. M., Pop, A., Iordache, F., Stanca, L., Predoi, G., and Serban, A. I. (2021). Oxidative stress mitigation by antioxidants - an overview on their chemistry and influences on health status. *Eur. J. Med. Chem.* 209, 112891. doi:10.1016/j.ejmech.2020.112891

Ratner, M. (2015). Biogen's early Alzheimer's data raise hopes, some eyebrows. *Nat. Biotechnol.* 33 (5), 438. doi:10.1038/nbt0515-438

Rowe, D., Mathers, S., Noel, K., and Rosenfeld, C. (2020). CuATSM phase 2a study confirms disease-modifying effects in patients with sporadic ALS observed in the phase 1 study (1338). *Neurology* 95 (15 Supplement), 1338.

Singh, P. N., Sabate, J., and Fraser, G. E. (2003). Does low meat consumption increase life expectancy in humans? *Am. J. Clin. Nutr.* 78 (3), 526s–532s. doi:10.1093/ajcn/78.3.526s

Sotgia, F., Martinez-Outschoorn, U. E., and Lisanti, M. P. (2011). Mitochondrial oxidative stress drives tumor progression and metastasis: Should we use antioxidants as a key component of cancer treatment and prevention? *BMC Med.* 9 (11), 62. doi:10.1186/1741-7015-9-62

Sotolongo, K., Ghiso, J., and Rostagno, A. (2020). Nrf2 activation through the PI3K/GSK-3 axis protects neuronal cells from Aβ-mediated oxidative and metabolic damage. *Alz. Res. Ther.* 12 (1), 13–22. doi:10.1186/s13195-019-0578-9

Spector, A. (1995). Oxidative stress-induced cataract: Mechanism of action. *FASEB J.* 9 (12), 1173–1182. doi:10.1096/fasebj.9.12.7672510

Tang, D., Chen, X., Kang, R., and Kroemer, G. (2021). Ferroptosis: Molecular mechanisms and health implications. *Cell Res.* 31 (2), 107–125. doi:10.1038/s41422-020-00441-1

Tang, M., Ji, C., Pallo, S., Rahman, I., and Johnson, G. V. W. (2018). Nrf2 mediates the expression of BAG3 and autophagy cargo adaptor proteins and tau clearance in an age-dependent manner. *Neurobiol. Aging* 63, 128–139. doi:10.1016/j.neurobiolaging.2017.12.001

von Otter, M., Landgren, S., Nilsson, S., Zetterberg, M., Celojevic, D., Bergström, P., et al. (2010). Nrf2-encoding NFE2L2 haplotypes influence disease progression but not risk in Alzheimer's disease and age-related cataract. *Mech. Ageing Dev.* 131 (2), 105–110. doi:10.1016/j.mad.2009.12.007

Wei, Z., Hao, C., Huangfu, J., Srinivasagan, R., Zhang, X., and Fan, X. (2021). Aging lens epithelium is susceptible to ferroptosis. *Free Radic. Biol. Med.* 167, 94–108. doi:10.1016/j.freeradbiomed.2021.02.010

Williams, J. R., Trias, E., Beilby, P. R., Lopez, N. I., Labut, E. M., Bradford, C. S., et al. (2016). Copper delivery to the CNS by CuATSM effectively treats motor neuron disease in SODG93A mice co-expressing the copper-chaperone-for-SOD. *Neurobiol. Dis.* 89, 1–9. doi:10.1016/j.nbd.2016.01.020

Wolff, S. P. (1994). Cataract and UV radiation. *Doc. Ophthalmol.* 88 (3-4), 201–204. doi:10.1007/bf01203674

Woo, S. Y., Kim, J. H., Moon, M. K., Han, S. H., Yeon, S. K., Choi, J. W., et al. (2014). Discovery of vinyl sulfones as a novel class of neuroprotective agents toward Parkinson's disease therapy. *J. Med. Chem.* 57 (4), 1473–1487. doi:10.1021/jm401788m

Wu, H., Yu, Y., David, L., Ho, Y. S., and Lou, M. F. (2014). Glutaredoxin 2 (Grx2) gene deletion induces early onset of age-dependent cataracts in mice. *J. Biol. Chem.* 289 (52), 36125–36139. doi:10.1074/jbc.m114.620047

Xing, K.-Y., and Lou, M. F. (2010). Effect of age on the thioltransferase (glutaredoxin) and thioredoxin systems in the human lens. *Invest. Ophthalmol. Vis. Sci.* 51 (12), 6598–6604. doi:10.1167/iovs.10-5672

Yildirim, Z., Ucgun, N. I., and Yildirim, F. (2011). The role of oxidative stress and antioxidants in the pathogenesis of age-related macular degeneration. *Clinics* 66 (5), 743–746. doi:10.1590/s1807-59322011000500006

Zhang, H., Liu, Y.-y., Jiang, Q., Li, K.-r., Zhao, Y.-x., Cao, C., et al. (2014). Salvianolic acid A protects RPE cells against oxidative stress through activation of Nrf2/HO-1 signaling. *Free Radic. Biol. Med.* 69, 219–228. doi:10.1016/j.freeradbiomed.2014.01.025

Zhang, S., Liu, H., Amarsingh, G. V., Cheung, C. C., Hogl, S., Narayanan, U., et al. (2014). Diabetic cardiomyopathy is associated with defective myocellular copper regulation and both defects are rectified by divalent copper chelation. *Cardiovasc. Diabetol.* 13 (1), 100. doi:10.1186/1475-2840-13-100

Zhang, W. C. (2019). microRNAs tune oxidative stress in cancer therapeutic tolerance and resistance. *Int. J. Mol. Sci.* 20 (23), 6094. doi:10.3390/ijms20236094

Zhao, Z., Chen, Y., Wang, J., Sternberg, P., Freeman, M. L., Grossniklaus, H. E., et al. (2011). Age-related retinopathy in NRF2-deficient mice. *PloS one* 6 (4), e19456. doi:10.1371/journal.pone.0019456

Zigman, S. (1995). Environmental near-UV radiation and cataracts. *Optom. Vis. Sci.* 72 (12), 899–901. doi:10.1097/00006324-199512000-00008